Inorganic Chemistry

pubs.acs.org/IC Article

Reductive Reactivity of the 4f⁷5d¹ Gd(II) Ion in {Gd^{II}[N(SiMe₃)₂]₃}⁻: Structural Characterization of Products of Coupling, Bond Cleavage, Insertion, and Radical Reactions

Amanda B. Chung, Austin J. Ryan, Ming Fang, Joseph W. Ziller, and William J. Evans*



Cite This: Inorg. Chem. 2021, 60, 15635-15645



ACCESS

III Metrics & More

Article Recommendations

s Supporting Information

ABSTRACT: The reductive reactivity of a Ln(II) ion with a nontraditional $4f'5d^1$ electron configuration has been investigated by studying reactions of the $\{Gd^{II}(N(SiMe_3)_2)_3]\}^-$ anion with a variety of reagents that survey the many reaction pathways available to this ion. The chemistry of both $[K(18-c-6)_2]^+$ and $[K(crypt)]^+$ salts (18-c-6=18-crown-6; crypt=2.2.2-cryptand) was examined to study the effect of the countercation. CS_2 reacts with the crown salt $[K(18-c-6)_2][Gd(NR_2)_3]$ (1) to generate the bimetallic $(CS_3)^{2-}$ complex $\{[K(18-c-6)](\mu_3-CS_3-\kappa S,\kappa^2S',S'')Gd(NR_2)_2]\}_2$, which contains two trithiocarbonate dianions that bridge Gd(III) centers and a potassium ion coordinated by 18-c-6. In contrast, the only crystalline product isolated from the reaction of CS_2 with the crypt salt $[K(crypt)][Gd(NR_2)_3]$ (2) is $[K(crypt)]\{(R_2N)_2Gd[SCS(CH_2)Si(Me_2)N(SiMe_3)-\kappa N,\kappa S]\}$, which has a CS_2 unit inserted into a cyclometalated amide ligand. Complexes 1 and 2 reductively couple pyridine to form bridging dipyridyl moieties, $(NC_5H_4-CS_3)$

 $\begin{array}{c} & & & & & & & & \\ & & & & & & & \\ & & & & & & \\ & & & & & & \\ & & & & & & \\ & & & & & & \\ & & & & & & \\ & & & & & & \\ & & & & & & \\ & & & & & & \\ & & & & & \\ & & & & & \\ & & & & & \\ & & & & & \\ & & & & & \\ & & & & \\ & & & & \\ & & & & \\ & & & & \\ & & & & \\ & & & & \\ & & & & \\ &$

 $C_5H_4N)^{2^-}$, that generate bimetallic complexes differing only in the countercation, $\{[K(18\text{-c-}6)(C_5H_5N)_2]\}_2\{[(R_2N)_3Gd]_2[\mu-(NC_5H_4-C_5H_4N)_2]\}$ and $[K(crypt)]_2\{[(R_2N)_3Gd]_2[\mu-(NC_5H_4-C_5H_4N)_2]\}$. Complexes 1 and 2 also show similar reactivity with (2,2,6,6-tetramethylpiperidin-1-yl) oxyl (TEMPO) to form the $(TEMPO)^-$ complexes $[K(18\text{-c-}6)][(R_2N)_3Gd(\eta^1\text{-ONC}_5H_6Me_4)]$ and $[K(crypt)][(R_2N)_3Gd(\eta^1\text{-ONC}_5H_6Me_4)]$, respectively. The first example of a bimetallic coordination complex containing a Bi–Gd bond, $[K(crypt)][(R_2N)_3Gd(BiPh_2)]$, was obtained by treating 2 with BiPh₃.

■ INTRODUCTION

The discovery that crystallographically characterizable complexes of rare-earth-metal Ln(II) ions were available for not only Eu, Yb, Sm, Tm, Dy, and Nd but also for Y, La, Ce, Pr, Gd, Tb, Ho, Er, and Lu^{1–7} opened up new opportunities in rare-earth reduction chemistry. The new Ln(II) ions generated by the reduction of $4\ell^p$ Ln(III) precursors were found to have $4\ell^p$ 5d¹ electron configurations rather than the traditional $4\ell^{p+1}$ Ln(II) configuration, and this offered the possibility of new reactivity patterns. 3-5

The new Ln(II) ions could be isolated across the lanthanide series from La to Lu as well as for Y in anions of the general formula $(Cp'_3Ln)^ (Cp'=C_3H_4SiMe_3)$, $^{2-7}$ but this tris(Cp') ligand set has not been ideal for isolating products of reactions with small molecules. 8,9 The $(Cp'_3Ln)^-$ complexes are reactive with most small-molecule reagents, but mixtures of products are often obtained that do not readily yield crystalline material suitable for a definitive crystallographic analysis of a single product.

The discovery that the new $4f'Sd^1$ Ln(II) ions could be isolated in the amide-ligated anions $[Ln(NR_2)_3]^-$ (R = SiMe₃; eqs 1 and 2) provided a different ligand set for investigating Ln(II) reactivity. Reactions of these isolated $[Ln(NR_2)_3]^-$

Ln(II) complexes with CO and $\rm N_2$ showed the amide ligand set to be advantageous in the isolation of reduced small molecules. $^{11-14}$

$$Ln^{|||}(NR_2)_3 + 2 \, 18 \cdot crown - 6 \qquad K/KC_8 \qquad O \qquad R_2N \qquad Ln^{||}(NR_2)_{3} + 2 \, 18 \cdot crown - 6 \qquad K/KC_8 \qquad O \qquad R_2N \qquad Ln^{||}(NR_2)_{3} + 2 \, 2 \cdot 2 \cdot crypt and \qquad K/KC_8 \qquad R_2N \qquad R$$

Received: July 26, 2021 Published: October 4, 2021





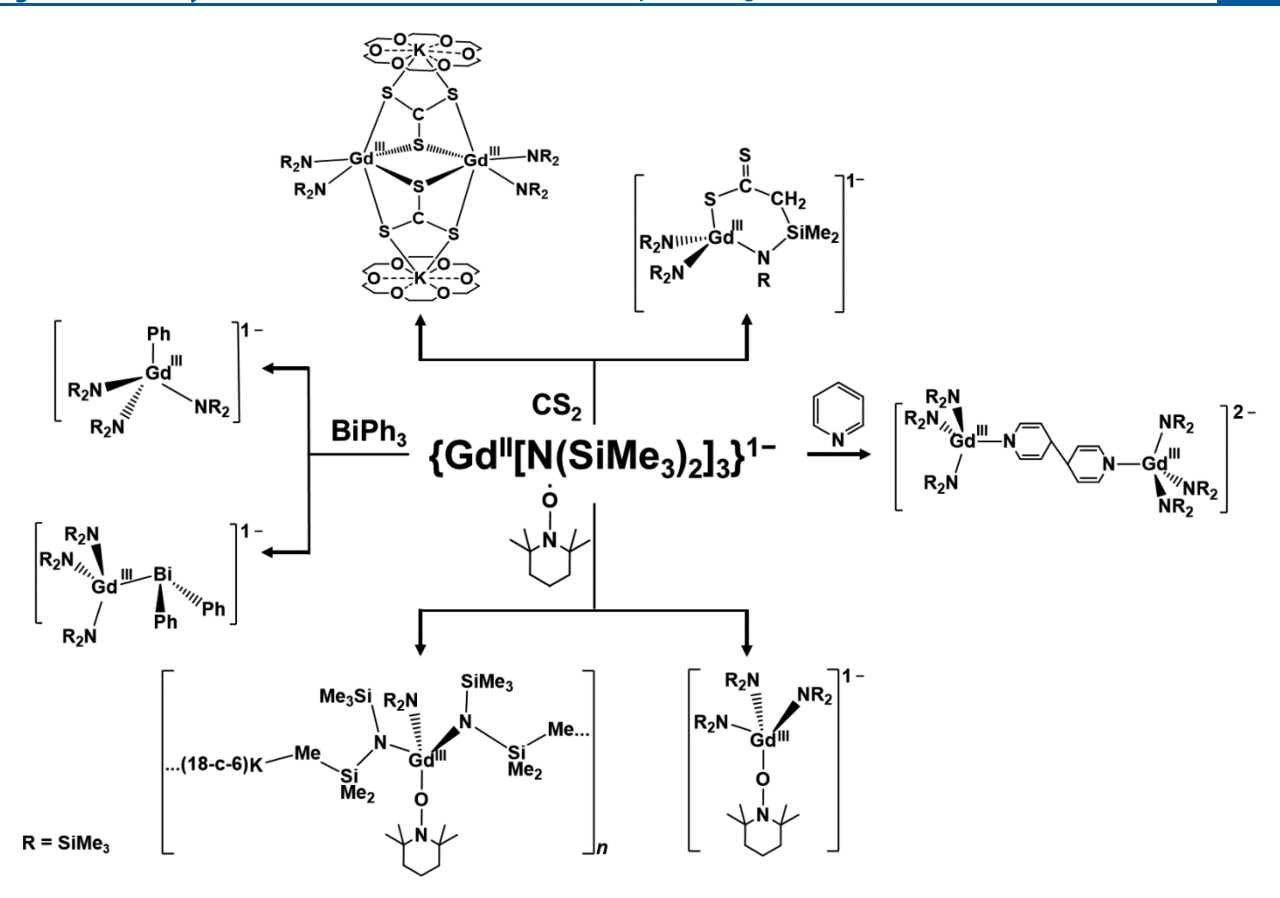


Figure 1. Overview of the reactivity of $[Gd(NR_2)_3]^-$.

Although the tris(amide) ligand set proved to be more favorable than the tris(cyclopentadienyl) complexes for small-molecule reactivity studies, it has not provided Ln(II) complexes across the series. Crystallographically characterized [Ln(NR₂)₃]⁻ complexes are known only for Nd, Sm, Eu, Gd, Tb, Dy, Ho, Er, Tm, Yb, Y, and Sc, and some of these examples are challenging to synthesize and have limited stability in solution. ^{10,11},13,15,16</sup> The [Gd(NR₂)₃]⁻ anion was chosen for this study because it is the member of the 4fⁿ5d¹ Ln(II) amide series most readily isolated as a crystalline solid. [Gd(NR₂)₃]⁻ has been crystallographically characterized as both [K(crypt)]⁺ and [K(18-c-6)₂]⁺ salts. ¹⁰ Since previous studies have shown that the identity of the cation can be crucial to the successful isolation of reaction products, ^{10,11} both salts were investigated.

We report here that both $[K(18\text{-c-6})_2][Gd(NR_2)_3]$ (1) and $[K(\text{crypt})][Gd(NR_2)_3]$ (2) react with a wide variety of reagents. However, since the Gd(III) products of these reactions are complexes of $4f^7$ Gd(III), which has a 7.9 μ_B magnetic moment, only the products that could be crystallographically characterized are reported here. As discussed in previous papers, 9,11 the products isolated from these reactions reflect the least soluble products of the reaction that are most prone to crystallize in a form analyzable by X-ray crystallography. Hence, the reaction products are representative of the types of reactions that can occur with Gd(II), but they should not be used to infer reaction mechanisms or even main reaction pathways.

■ RESULTS AND DISCUSSION

The reactivity of the $[Gd(NR_2)_3]^-$ complex was examined with a variety of reagents, as shown in Figure 1.

The broad range of reagents was chosen to survey multiple different reaction pathways for Gd(II) and to compare with prior studies of reductive rare-earth chemistry. As was mentioned above, prior studies had been done with CO^{11} and $\mathrm{N_2}^{14}$ and the chemistry of CO_2 with the *in situ* amide system of yttrium, i.e. $\mathrm{Y(NR_2)_3/K}$, had already been studied. Reactions with NO have not given identifiable products. In this study, reagents beyond these common small-molecule reagents were examined.

Carbon Disulfide. CS_2 was chosen as a reagent since it had been previously studied with complexes of the traditional $4f^6$, $4f^7$, and $4f^{14}$ ions Sm(II), Eu(II), and Yb(II), respectively. A variety of products were identified from these reactions, including $(CS_2)^{2-18,19}$ coupled $(SCS-CS_2)^{2-20,21}$ and $(SC \equiv CS)^{2-19}$ as well as the potassium salts K_2CS_3 , $K_2C_2S_4$, and $K_2C_3S_5$. CS_2 reduction has also been studied with actinide reducing reagents, and complexes containing trithiocarbonate, $(CS_3)^{2-}$, have been isolated. CS_3 0 was also of interest, since an *in situ* CS_3 1 was been isolated. CS_3 2 reaction had previously generated crystals of a trithiocarbonate, CS_3 2 (CS_3 3)2 (CS_3 4)2 (CS_3 4)2 (CS_3 5)3 (CS_3 6)3 (CS_3 6)3 (CS_3 7)3 (CS_3 6)3 (CS_3 7)3 (CS_3 8)3 (CS_3 8)3 (CS_3 9)3 (CS_3 9 (CS_3 9)3 (CS_3 9)3 (CS_3 9 (CS_3 9)3 (CS_3 9)3 (CS_3 9 (CS_3 9)3 (C

A Trithiocarbonate from CS₂ and 1. The dropwise addition of excess CS₂ to a dark blue solution of the 18-c-6 complex $[K(18\text{-c-}6)_2][Gd(NR_2)_3]$ (1) dissolved in Et₂O at -35 °C under Ar immediately formed a dark yellow solution. Within 24 h, small amounts of light yellow crystals grew on top of a red oil that solidified at -35 °C. The yellow crystals were characterized by X-ray diffraction as the trithiocarbonate complex $\{[K(18\text{-c-}6)](\mu_3\text{-CS}_3\text{-}\kappa S,\kappa^2 S',S'')[Gd(NR_2)_2]\}_2$ (3; Figure 2 and eq 3). Attempts to crystallize the red oil have

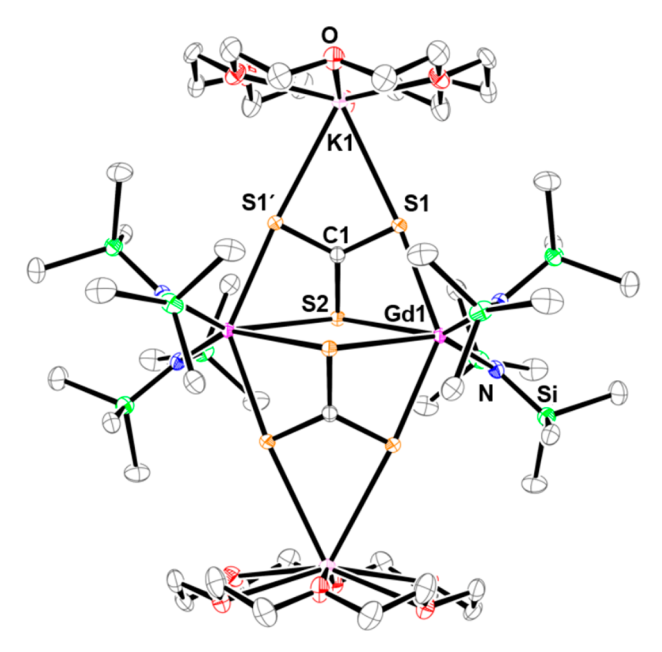


Figure 2. Representation of $\{[K(18-c-6)](\mu_3-CS_3-\kappa S,\kappa^2S',S'')[Gd-(NR_2)_2]\}_2$ (3) with atomic displacement parameters drawn at the 50% probability level. Hydrogen atoms are omitted for clarity.

so far been unsuccessful, although its IR and UV-visible spectra are very similar to those of the yellow crystals (see the Supporting Information). The stoichiometry with respect to CS_2 did not affect the outcome of the reaction: similar results were observed from reactions of 1 with 1 equiv and excess CS_2 .

$$[K(chelate)_x][Gd^{[l]}(NR_2)_3] \xrightarrow{xs \ CS_2} \\ R = SiMe_3; \ 18-c-6 = 18-crown-6; \\ crypt = 2.2.2-cryptand \\ \begin{bmatrix} K(crypt) \end{bmatrix} \xrightarrow{SiMe_2} \\ R_2N \xrightarrow{Gd^{[l]}(NR_2)_3} \\ R_2N \xrightarrow{R_2N} \\ R_2N \xrightarrow{$$

Complex 3 is a tetrametallic compound that contains two trithiocarbonate dianions $(CS_3)^{2-}$ with each sulfur involved in a bridge between two metals. It crystallizes in the monoclinic $P2_1/c$ space group with one formula unit per unit cell. One sulfur from each $(CS_3)^{2-}$ ligand bridges two Gd(III) ions, each

ligated by two $(NR_2)^-$ ligands. The other two sulfur atoms bridge a Gd(III) ion and a potassium ion bound to an 18-c-6 ligand. This type of κ^3 $(CS_3)^2$ has been observed previously in the extended 3D polymeric structure of $(K_2CS_3)_5(DMSO)_{12}$, in which each sulfur bridges three potassium ions and each potassium is coordinated by three thiocarbonate sulfur atoms and three DMSO ligands²² (Figure 3). It has also been found in $(RO)_4U(CS_3)[(K(18\text{-crown-6})]_2$ $(R = Si(OCMe_3)_3)^{24}$ and in $(RR'N)_2Fe(CS_3)[K(18\text{-crown-6})]_2$ $(R = SiMe_3; R' = 2,6\text{-diisopropylphenyl})^{25}$ (Figure 3). The U and Fe structures differ from 3 in that there are two $[K(18\text{-crown-6})]^+$ units coordinating to the κ^3 $(CS_3)^{2-}$ and only one other metal (U, Fe) rather than one potassium and two Gd as in 3. The product of the *in situ* $Y(NR_2)_3/KC_8/18\text{-c-6}/CS_2$ reaction is also shown in Figure 3.

In Table 1, the metrical parameters on 3 are compared with those of the related yttrium complex {[K(18-c-

Table 1. Selected Metrical Parameters for $\{[K(18\text{-c-6})](\mu_3\text{-CS}_3\text{-}\kappa S,\kappa^2 S',S'')[Gd(NR_2)_2]\}_2$ (3) and $\{[K(18\text{-c-6})_2(THF)_2]_2[(R_2N)_2Y(\mu\text{-CS}_3\text{-}\kappa^2 S,S')]_2\}(18\text{-c-6})$ (Å, deg)

{[K(18-c-6)](μ_3 -CS ₃ - κ S, κ ² S',S'') [Gd(NR ₂) ₂]} ₂		$ \begin{array}{c} \{[K(18\text{-c-6})_2(THF)_2]_2[(R_2N)_2Y(\mu\text{-}\\CS_3\text{-}\kappa^2S,S')]_2\}(18c6) \end{array} $	
Gd1-N1	2.285(4)	Y1-N1	2.260(2)
		Y1-N2	2.258(2)
Gd1-S1	2.8350(11)	Y1-S1	2.8055(8)
Gd1-S1'	2.8349(11)	Y1-S3	2.7930(7)
Gd1-S2	3.0180(9)	Y1-S2	2.9442(7)
S1-C1	1.712(3)	S1-C13	1.702(3)
S2-C1	1.718(7)	S2-C13	1.731(3)
S1'-C1	1.712(3)	S3-C13	1.702(3)
S1-C1-S1'	120.8(4)	S1-C13-S3	122.38(16)
S1-C1-S2	119.53(19)	S1-C13-S2	119.25(16)
S1'-C1-S2	119.53(19)	S3-C13-S2	118.23(16)

6)₂(THF)₂]₂[(R₂N)₂Y(μ -CS₃- κ ²S,S')]₂}(18-c-6) (Figure 3), isolated from an *in situ* Y(NR₂)₃/KC₈/18-c-6/CS₂ reaction (see the Supporting Information). Although the structures differ in that potassium is not coordinated to the (CS₃)²⁻ ion in the yttrium complex, the metrical parameters are very similar after taking into account that the ionic radius of Y(III) is approximately 0.03–0.04 Å shorter than that of Gd(III).²⁶

Despite the two types of sulfur bridges in 3, i.e. Ln–S–Ln and Ln–S–K, the metrical parameters of the $(CS_3)^{2-}$ ligands are quite uniform. The S–C–S angles span a small range: 119.1(2), 120.8(4), and 119.1(2)°. The 1.712(3) (C1–S1), 1.712(3) (C1–S1'), and 1.718(7) Å (C1–S2) C–S distances are between the values typical for a C–S single bond, 1.819 Å, and a C=S double bond, 1.671 Å, 27 which suggests that the

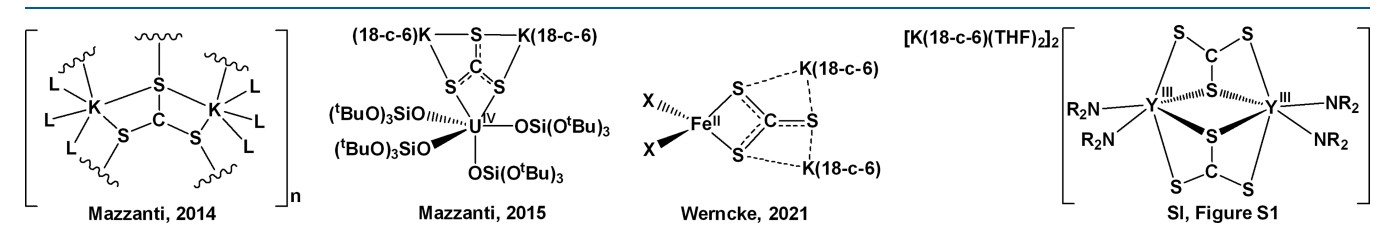


Figure 3. $(CS_3)^{2-}$ complexes: $[(K_2CS_3)_5(L)_{12}]_n$ (L = DMSO), 22 $\{U[OSi(O^tBu)_3]_4(\mu_3-\kappa^2:\kappa^2CS_3)K_2(18-c-6)_2\}$, 24 $[K(18-c-6)]_2[X_2Fe(\eta^2-CS_3)]$ $(X = N(Dipp)SiMe_3$, Dipp = 2,6-diisopropylphenyl), 25 and $\{[K(18-c-6)_2(THF)_2]_2[(R_2N)_2Y(\mu-CS_3-\kappa^2S_5S')]_2\}(18-c-6)$ (Supporting Information) $(R = SiMe_3)$.

charge is delocalized across all three C–S bonds. These bond distances are similar to those in $[\{((^{\mathrm{Ad}}\mathrm{ArO})_3\mathrm{N})\mathrm{U}\}_2(\mu\text{-CS}_3-\kappa S,\kappa S')]$,with C–S bond distances of 1.724(4), 1.707(4), and 1.710(4) Å. 23 The metrical parameters of the (CS $_3$) $^{2-}$ unit in $\{[K(18\text{-c-}6)_2(\mathrm{THF})_2]_2[(R_2\mathrm{N})_2\mathrm{Y}(\mu\text{-CS}_3-\kappa^2 S,S')]_2\}(18\text{-c-}6)$ are similar to those in 3, even though potassium is not bound. This indicates that the $[K(18\text{-c-}6)]^+$ ions are not significantly perturbing the core structure in 3.

In 3, the planar Gd, Gd', S2, S2' quadrilateral is perpendicular to the plane defined by C1, S2, C1', and S2'. $\{[K(18-c-6)_2(THF)_2]_2[(R_2N)_2Y(\mu-CS_3-\kappa^2S,S')]_2\}(18-c-6) \text{ has}$ a similarly symmetrical arrangement, but the 2.9442(7) Å Y1-S2 distance differs slightly from the 2.9814(7) Å Y1-S2' distance. In 3, the quadrilateral is rhombic with 3.0189(9) Å Gd1-S2 and Gd1-S2' distances. All of the other Ln-N and Ln-S distances in 3 and the yttrium analogue are similar when the difference in ionic radii is taken into account. The 2.8350(11) Å Gd1-S1 and 2.8349(11) Å Gd1-S1' distances in 3 for the sulfur atoms bridging to potassium are shorter than that in the Gd-S-Gd bridging unit, 3.0180(9) Å. The 113.8(5)° Gd-S-Gd angle is also more acute than the 168.5(5)° Gd-S-K angle. The 2.285(4) Å Gd-N(NR₂) distances in 3 are only slightly longer than the 2.230(6) and 2.244(6) Å analogues in the complex with simple (SR) bridging ligands in $[(R_2N)_2Gd(\mu-SBu^t)]_2$.

A CS₂ Insertion Product from 2. Like 1 above, the crypt complex $[K(crypt)][Gd(NR_2)_3]$ (2) reacts immediately with CS₂ with 2 with a color change from dark blue to yellow in THF. However, the crystalline product isolated in this case was $[K(crypt)]\{(R_2N)_2Gd[SCS(CH_2)Si(Me_2)N(SiMe_3)-\kappa N,\kappa S]\}$ (4; Figure 4 and eq 3).

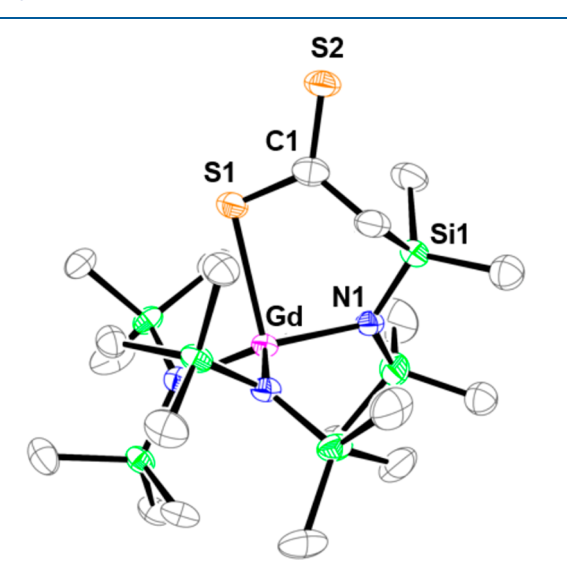


Figure 4. Representation of the anion of $[K(crypt)]\{(R_2N)_2Gd-[SCS(CH_2)Si(Me_2)N(SiMe_3)-\kappa N,\kappa S]\}$ (4) with atomic displacement parameters drawn at the 50% probability level. Hydrogen atoms are omitted for clarity.

Complex 4 formally appears to be the product of insertion of CS_2 into the Gd-C bond of the cyclometalated amide unit " $\{(R_2N)_2Gd[(CH_2SiMe_2)N(SiMe_3)-\kappa C,\kappa N]\}^-$ ". Cyclometalation of $N(SiMe_3)_2$ ligands is a common reaction for this ligand, ^{29–44} and examples of C-H bond activation have been observed previously in reductive Ln(II) chemistry. ^{45–47} Hence, it is conceivable that the cyclometalated product is generated

in this reaction. The only other known lanthanide-based CS_2 insertion product is an Yb(II) dithiocarbamate, Yb(S_2CNR_2)₂, which was obtained from the reaction of [Yb(NR_2)₂(OEt_2)₂] with CS_2 but was not crystallographically characterized.⁴⁸

No examples of insertion of CS_2 into a Gd-C bond of a cyclometalated amide were found in the literature for comparison with 4. Complex 4 crystallizes in the monoclinic $P2_1/n$ space group with one formula unit per unit cell. The 1.726(4) Å S1-C bond length is shorter than the typical C-S bond length of 1.819 Å, whereas the 1.659(3) Å C-S2 bond is close to that of a C=S double bond, 1.671 Å. 27 The 2.288(3) Å Gd-N1 cyclometalated nitrogen bond length is indistinguishable from the 2.286(2) Å Gd-N3 and 2.292(2) Å Gd-N2 terminal amide distances. All of these Gd-N distances are similar to those in 3. The 2.7490(9) Å Gd-S1 bond length in 4 is shorter than the Gd-S bonds of 3, which involves sulfur bridging two metal atoms. The newly formed C-C bond distance is 1.506(5) Å, in the typical single-bond range.

Pyridine Reductive Coupling from 1 and 2. Pyridine is another reagent that has been examined with other low-oxidation-state lanthanide and actinide complexes; thus, there is precedent for investigating its reactivity with Gd(II). Reductive coupling has been observed with Sm(II), 49 Tm-(II), 50,51 U(II), 52 and Th(III). Reductive coupling with transition metals is also known.

Dropwise addition of excess pyridine to a dark blue solution of 1 in Et₂O at -35 °C in an argon-filled glovebox immediately formed a light pink solution. This solution was layered into hexanes, and the product crystallized at -35 °C within 24 h as pink crystals. X-ray diffraction revealed that these crystals were the reductively coupled pyridine complex $\{[K(18\text{-c-}6)-(NC_5H_5)_2]\}_2\{[(R_2N)_3Gd]_2[\mu-(NC_5H_4-C_5H_4N)_2]\}$ (5; Figure 5 and eq 4) with a pyridine-ligated potassium 18-c-6 countercation.

$$[K(18-c-6)(py)_{2}]_{2} \begin{bmatrix} R_{2}N_{\infty}^{2N} & NR_{2} \\ R_{2}N_{\infty}^{2N} & NR_{2} \end{bmatrix}$$

$$[K(chelate)_{3}][Gd^{\parallel}(NR_{2})_{3}] - 35 ^{\circ}C$$

$$R = SiMe_{3}; 18-c-6 = 18-crown-6;$$

$$crypt = 2.2.2-cryptand$$

$$[K((crypt))_{2}]_{2} \begin{bmatrix} R_{2}N_{\infty}^{2N} & NR_{2} \\ R_{2}N_{\infty}^{2N} & NR_{2} \end{bmatrix}$$

$$(4)$$

$$R_{2}N_{\infty}^{2N} & NR_{2} \\ R_{2}N_{\infty}^{2N} & NR_{2} \end{bmatrix}$$

$$R_{2}N_{\infty}^{2N} & NR_{2} \\ R_{2}N_{\infty}^{2N} & NR_{2} \\ R_{2}N_{\infty}^{2N} & NR_{2} \end{bmatrix}$$

A reaction analogous to the pyridine/1 reaction was also explored with a dark blue solution of 2 in THF, and this afforded the similarly coupled pyridine complex [K-(crypt)]₂{[(NR₂)₃Gd]₂[μ -(NC₅H₄-C₅H₄N)]}₂ (6; Figure S6 and eq 4), which differed only in the countercation. Complex 6 crystallizes with two molecules of the bimetallic Gd complex in the unit cell along with four [K(crypt)]⁺ countercations and six THF molecules in the crystal lattice. For 6, the data were not of high enough quality for a detailed structural discussion.

Selected bond distances of **5** are given in Table 2. Complex **5** crystallizes in the monoclinic $P2_1/n$ space group with one formula unit per unit cell. The C–C bonds C2–C3 (1.518(8) Å), C4–C3 (1.498(8) Å), and C3–C3′ (1.565(10) Å) are typical C–C single-bond lengths.²⁷ The C1–C2 (1.342(8) Å) and C5–C4 (1.335(8) Å) distances are typical for C=C bonds.²⁷ The 2.287(4) Å Gd–N[μ -(NC₅H₄-C₅H₄N)] distance in **5** is close to the 2.298(4)–2.337(4) Å range of Gd–N(amide) single-bond distances. In comparison, the recently

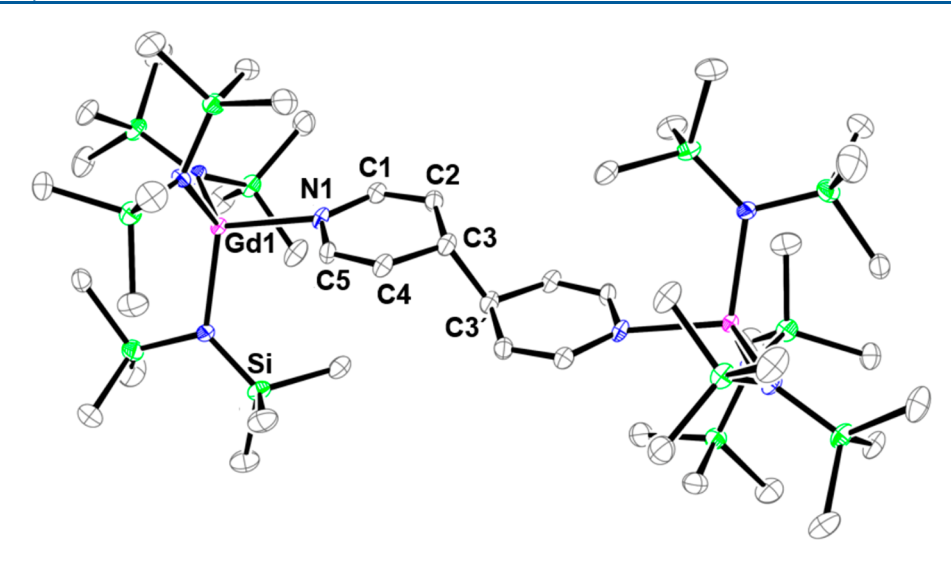


Figure 5. Representation of $\{[K(18-c-6)(NC_5H_5)_2]\}_2\{[(R_2N)_3Gd]_2[\mu-(NC_5H_4-C_5H_4N)_2]\}$ (5) with atomic displacement parameters drawn at the 50% probability level. Hydrogen atoms and $[K(18-c-6)(NC_5H_5)_2]^+$ are omitted for clarity.

Table 2. Selected Bond Distances (Å) for 5

Gd-N1(py)	2.287(4)
Gd-N _{amide}	2.298(4), 2.334(5), 2.337(4)
N1-C1	1.395(7)
N1-C5	1.392(7)
C1-C2	1.342(8)
C5-C4	1.335(8)
C2-C3	1.518(8)
C4-C3	1.498(8)
C3-C3'	1.565(10)

reported uranium complex $[K(crypt)]_2\{[(R_2N)_3U]_2[\mu-(NC_5H_4-C_5H_4N)]\}^{52}$ has an average 2.385(5) Å U–N(amide) distance that is similar to the U–N[μ -(NC $_5H_4$ -C $_5H_4$ N)] distance of 2.404(7) Å. The longer uranium distances are consistent with the fact that the Shannon radius of U(III) is 0.087 Å larger than that of Gd(III). The C3–C3′ bond distance of 1.565(10) Å for 5 is within error equal to the uranium complex distance, which was 1.570(17) Å. These distances are also consistent with a single bond and are close to the range of 1.559(4)–1.563(6) Å distances reported for iron, samarium, thulium, so, and thorium complexes featuring reductively coupled pyridines.

Reduction of (2,2,6,6-Tetramethylpiperidin-1-yl)oxyl (TEMPO) by 1 and 2. To examine the radical reactivity of the $4f^7Sd^1$ ion, TEMPO reactions were studied. When an orange solution of TEMPO in Et_2O at -35 °C was added to a dark blue solution containing 1 in Et_2O at -35 °C, the solution turned light pink. Colorless crystals were obtained from this solution layered under hexanes and were characterized by X-ray diffraction to be $\{[(18-c-6)K][(\mu-Me_3Si)(Me_3Si)N]_2[Gd-(NR_2)(\eta^1-ONC_5H_6Me_4)]\}_n$ (7; Figure 6 and eq 5). In the solid state, this complex has an extended structure generated by interactions on either side of the $[K(18-c-6)]^+$ cation with silylmethyl groups of the $(NR_2)^-$ ligands (Figure 7).

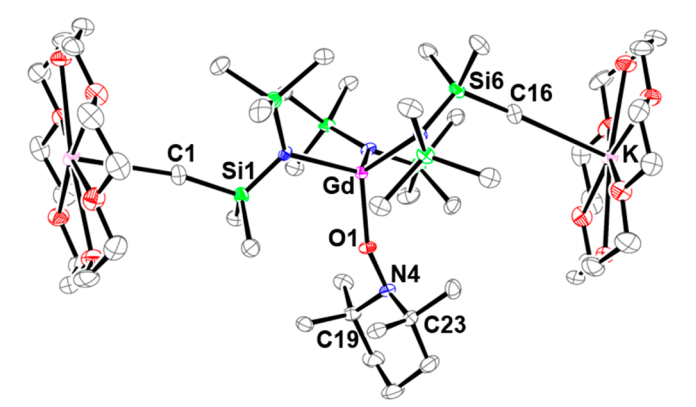


Figure 6. Representation of {[(18-c-6)K][(μ -Me₃Si)(Me₃Si)N]₂[Gd-(NR₂)(η ¹-ONC₅H₆Me₄)]}_n (7) plus an additional K(18-c-6)]⁺ unit to show the connectivity of the polymer, with atomic displacement parameters drawn at the 50% probability level. Hydrogen atoms are omitted for clarity.

$$[K(\text{chelate})_{x}][Gd^{\parallel}(NR_{2})_{3}] \xrightarrow{O} - 35 \text{ °C}$$

$$R = \text{SiMe}_{3}; 18 \text{ ·c-} 6 = 18 \text{ ·crown-} 6; \text{ crypt} = 2.2.2 \text{ ·cryptand}$$

$$R = \text{SiMe}_{3}; 18 \text{ ·c-} 6 = 18 \text{ ·crown-} 6; \text{ crypt} \\ x = 1$$

$$R_{2} \text{ is a constant of the late} = \text{ is constant of the late} = \text{ crypt} \\ x = 1$$

$$R_{2} \text{ is a constant of the late} = \text{ crypt} \\ x = 1$$

$$R_{2} \text{ is a constant of the late} = \text{ crypt} \\ R_{2} \text{ is a constant of the late} \\ R_{2} \text{ is a constant of the late} \\ R_{2} \text{ is a constant of the late} \\ R_{2} \text{ is a constant of the late} \\ R_{2} \text{ is a constant of the late} \\ R_{2} \text{ is a constant of the late} \\ R_{2} \text{ is a constant of the late} \\ R_{2} \text{ is a constant of the late} \\ R_{2} \text{ is a constant of the late} \\ R_{2} \text{ is a constant of the late} \\ R_{2} \text{ is a constant of the late} \\ R_{2} \text{ is a con$$

Each Gd(III) center is attached to two bridging $(NR_2)^-$ groups, one terminal $(NR_2)^-$ group, and the TEMPO anion. The reaction of **2** with TEMPO in THF afforded the analogous complex $[K(crypt)(THF)][(R_2N)_3Gd(\eta^1-ONC_5H_6Me_4)]$ (**8**; Figure 8 and eq 5), but with the $[K(crypt)(THF)]^+$ countercation, ^{55,56} an extended structure was not formed.

Both 7 and 8 crystallize in the monoclinic $P2_1/n$ space group, but an extended structure is found only in 7. Complexes 7 and 8 contain η^1 -TEMPO⁻ anions like those in $(\eta^5$ -

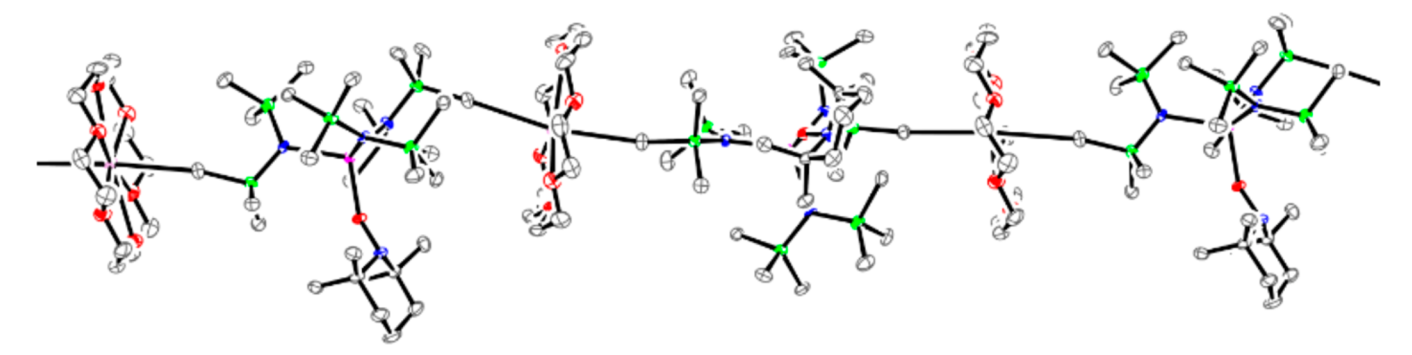


Figure 7. Representation of the extended structure of $\{[(18\text{-c-6})K][(\mu\text{-Me}_3Si)(Me_3Si)N]_2[Gd(NR_2)(\eta^1\text{-ONC}_5H_6Me_4)]\}_n$ (7) with atomic displacement parameters drawn at the 50% probability level. Hydrogen atoms are omitted for clarity.

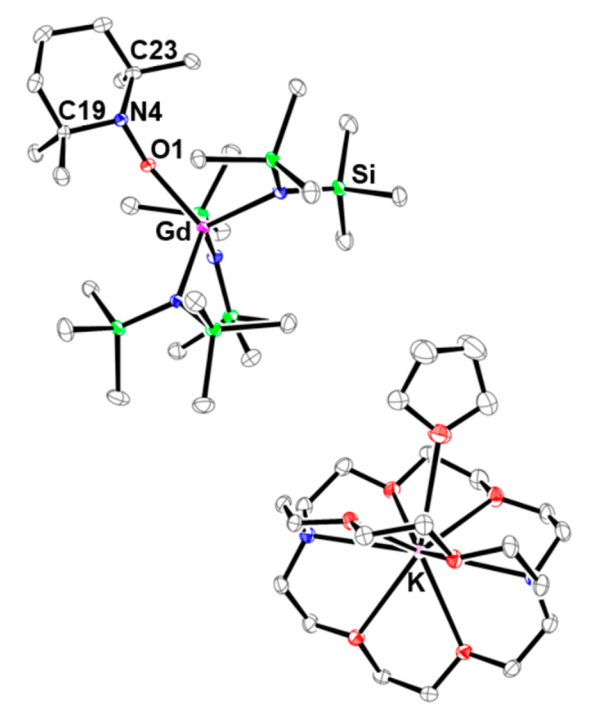


Figure 8. Representation of $[K(crypt)(THF)][(R_2N)_3Gd(\eta^1-ONC_5H_6Me_4)]$ (8) with atomic displacement parameters drawn at the 50% probability level. Hydrogen atoms are omitted for clarity.

 $C_5Me_5)_2Th(Me)(\eta^1-ONC_5H_6Me_4).^{57}$ The Gd-O(TEMPO) distances in 7 and 8, 2.1313(18) and 2.1342(10) Å,

Table 3. Selected Metrical Parameters for 7 and 8 (Å, deg)

	7	8
$Gd-N_{amide}$	2.333(2), 2.359(2), 2.366(2)	2.3361(12), 2.3638(12), 2.3734(12)
Gd-O1	2.1313(18)	2.1342(10)
O1-N4	1.439(3)	1.4386(15)
O1-N4-C19	108.98(19)	109.46(10)
O1-N4-C23	108.9(2)	109.26(10)

respectively (Table 3), are similar to those in the thorium complex, which is consistent with the fact that Gd(III) and Th(IV) have similar ionic radii. The O1–N4 distances and the O–N–C angles in both 7 and 8 are typical for a TEMPO anion. S7–62 Similarly, the sums of the angles around the nitrogen center, 335.8° for 7 and 336.8° for 8, are consistent

The extended structure of 7 has precedent in that $K\cdots$ Me(SiMe₃) linkages have been observed before with [K(18-c-6)]⁺ cations, ⁶³⁻⁶⁶ but not on both sides of the potassium crown entity to our knowledge. The six donor oxygen atoms of 18-c-6 are planar to within 0.1721 Å, and the potassium is 0.1549 Å out of the plane. The $K\cdots C(Me_3Si)$ distances are 3.130(3) and 3.172(3) Å, with the $C\cdots K$ vector making an 85.7° angle for C(1) and a 104.8° angle for C(16) with the plane of the six oxygen donor atoms of 18-c-6.

Formation of a Gd–Bi Complex from 2 and BiPh₃. The reaction of BiPh₃ with the Gd(II) complexes was investigated to determine if there was any connection between the previously reported reaction of the Sm(II) complex $(C_5\text{Me}_5)_2\text{Sm}$ with BiPh₃ that forms $[(C_5\text{Me}_5)_2\text{Sm}]_2(\mu-\eta^2:\eta^2-\text{Bi}_2)$ along with $(C_5\text{Me}_5)_2\text{SmPh}$. Addition of solid 1 to a solution of BiPh₃ in Et₂O at room temperature results in an immediate color change from colorless to orange. Crystallization at -35 °C under hexanes yielded an orange-brown oil and blue crystals. The crystals were identified by X-ray crystallography as the Bi–C(Ph) cleavage product $[K(18-c-6)_2][\text{PhGd}(NR_2)_3]$ (9; Figure 9 and eq 6).

$$\begin{bmatrix} K(18-c-6)_{2} \\ Et_{2}O \\ BiPh_{3} \\ = SiMe_{3}; \ 18-c-6 = 18-crown-6; \\ crypt = 2.2.2-cryptand \end{bmatrix} \underbrace{ \begin{bmatrix} K(18-c-6)_{2} \\ BiPh_{3} \\ = SiMe_{3}; \ 18-c-6 = 18-crown-6; \\ crypt \\ x = 1 \end{bmatrix} \underbrace{ \begin{bmatrix} K(18-c-6)_{2} \\ R_{2}N \\$$

The same reaction performed with 2 produced similar color changes, but crystallization at $-35\,^{\circ}\text{C}$ yielded bright green crystals as well as an orange oil. X-ray diffraction revealed that the green crystals were $[K(\text{crypt})][(Ph_2Bi)Gd(NR_2)_3]$ (10; Figure 10 and eq 6), the bismuth product expected after one Bi–C(Ph) cleavage reaction. The only other crystallographically characterized complex containing bismuth and gadolinium is the Zintl cluster $[K(\text{crypt})]_4[Gd@Pb_4Bi_9],^{68}$ which has 13 cage atoms around the Gd. Five of the cage atoms were identified by crystallography as Bi, but the identity of the other eight cage atoms could not be determined due to the similar atomic numbers of Pb and Bi. Hence, 10 provides the first example of a simple coordination complex with a single Gd–Bi bond. Complexes containing f-element to Bi bonds are rare in general. 67,69 The structure of $[K(\text{crypt})][\text{BiPh}_2]$ (Figure S13)

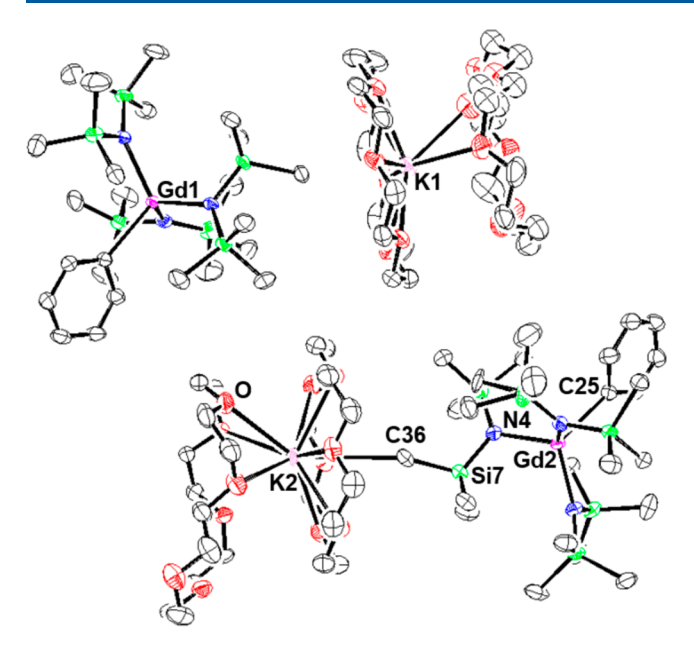


Figure 9. Representation of the two forms of $[K(18-c-6)_2][PhGd-(NR_2)_3]$ (9) with atomic displacement parameters drawn at the 50% probability level. Hydrogen atoms and disorder in SiMe₃ groups are omitted for clarity.

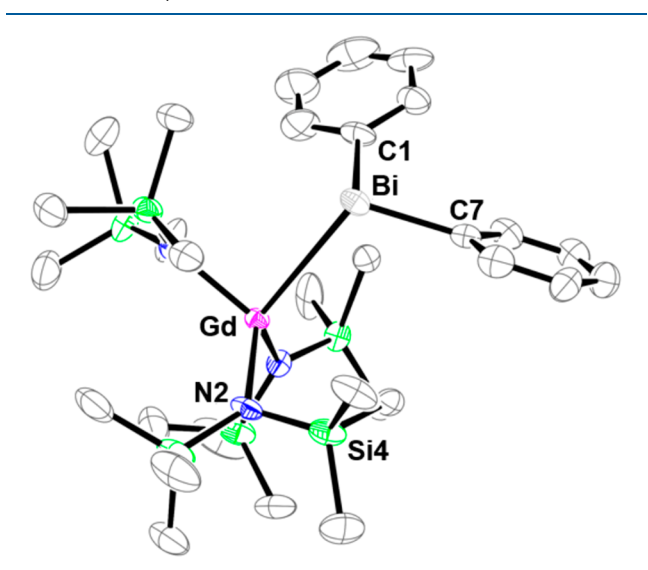


Figure 10. Representation of $[K(crypt)][(Ph_2Bi)Gd(NR_2)_3]$ (10) with atomic displacement parameters drawn at the 50% probability level. Hydrogen atoms, the disordered SiMe₃ group, and $[K(crypt)]^+$ are omitted for clarity.

was also identified from this reaction system, which is summarized in eq 6. We found no other structures of the $(BiPh_2)^-$ anion in a CCDC search.

The phenyl complex **9** crystallizes with an unusual structure that has two different molecules of $[K(18\text{-c-}6)_2][PhGd(NR_2)_3]$ per unit cell. One anionic $[PhGd(NR_2)_3]^-$ unit is well separated from the $[K(18\text{-c-}6)_2]^+$ cation. The other shows a 3.391(5) Å $K\cdots C(methyl)$ contact between an $(NR_2)^-$ ligand and the $[K(18\text{-c-}6)_2]^+$ cation. Despite the different structures, the metrical parameters around the two Gd ions in the anion are the same within error. For example, the Gd–N distances range from 2.30(5) to 2.325(4) Å in the isolated anion and from 2.313(4) to 2.326(4) Å in the anion with the methyl to potassium interaction. The Gd–C(Ph) distance is 2.525(5) Å

in the isolated anion and 2.521(5) Å in the anion with the K··· Me connection. The known eight-coordinate $(C_5Me_5)_2SmPh(THF)$ complex, produced by a similar reaction protocol with BiPh₃, displays a Sm–C(Ph) bond length of 2.511(8) Å similar to that observed in 9 despite the difference in coordination number of the two complexes and the 0.026 Å smaller size of Gd(III) in comparison to Sm(III).³⁴

One sample of 10 was found to crystallize in the triclinic $P\overline{1}$ space group, and a subsequent crystallization gave 10 in the monoclinic P2₁/c space group. In both cases there is only one formula unit per unit cell. The molecular parameters are similar in both cases, and data from only the triclinic crystal are discussed here (see the Supporting Information for monoclinic data). The structure of 10 has an irregular pseudotetrahedral coordination environment around the Gd ion generated by three NR₂ ligands and one BiPh₂ ligand with 88.33(16)-124.00(16)° N-Gd-N and N-Gd-Bi angles. There is also one Me₃Si group that is oriented toward Gd with a 108.8(3)° Gd-N(2)-Si(4) angle that is more acute than the other Gd-N-Si angles, which range from 116.0(3) to 131.7(4)°. The three-coordinate bismuth atom has 96.9(2) and 110.4(2)° Gd-Bi-C(Ph) angles and a 98.0(3)° C(Ph)-Bi-C(Ph) angle, which leaves a large amount of open space in the coordination sphere, as is typical for bismuth. 70,71 The 3.3516(5) Å Gd-Bi bond in **10** is similar to the 3.3208(4) $\text{Å U-Bi bond in } \{(Me_3Si)_2Bi]U(TrenDMBS)\} \text{ (TrenDMBS = }$ N(CH₂CH₂NSiMe₂Bu^t)₃)⁶⁹ when the 0.05 Å larger ionic radius of Gd(III) versus U(IV) is considered. The similarities in metrical parameters extend to the M-N(amide) bonds with distances ranging from 2.286(6) to 2.296(6) Å for 10 vs 2.232(6) to 2.247(6) Å in $\{(Me_3Si)_2Bi\}U(TrenDMBS)\}$.

Ph–Sn Cleavage with Ph₄Sn. To further explore the reductive cleavage of Ph–main-group-element bonds, the reaction of **2** with SnPh₄ was examined. However, the only crystallographically characterizable product was [K(crypt)]- $[SnPh_3](THF)$ (Figure S14). The X-ray crystal structures of $[K(18\text{-}crown-6)]\{SnPh_3]$, 72 $[Ba(18\text{-}crown-6)(HMPA)_2]$ - $[SnPh_3]_2$, 73 and $(Me_2NCH_2CH_2)_2NMe)LiSnPh_3$ have been previously reported.

CONCLUSION

Both $[K(18-c-6)_2][Gd(NR_2)_3]$ (1) and the crypt analogue $[K(crypt)][Gd(NR_2)_3]$ (2) can perform a variety of reductive reactions and provide new synthetic pathways to Gdcontaining compounds. The reactions with pyridine show reductive coupling reactivity for the Gd(II) ion, while the reactions with BiPh3 show that reductive cleavage is viable in this case with a Bi-Ph bond. With CS2, the reactions show a combination of cleavage and coupling reactions, while the reaction with TEMPO reinforces the radical nature of Gd(II). In some cases, the reductive reactivity results in loss of a $(NR_2)^-$ ligand to form products of the $[(R_2N)_2Gd]^+$ cation, but in other cases, anionic complexes of Gd(NR₂)₃ are formed that retain all of the amide ligands in the starting materials. With some reagents, the $[K(18-c-6)_2]^+$ and $[K(crypt)]^+$ salts give different products, and with others, both species give the same reductive chemistry. Clearly extensive reactivity is available through Gd(II), and the details of the reductions can be very influential in terms of product isolation.

■ EXPERIMENTAL SECTION

All manipulations and syntheses described below were conducted with the rigorous exclusion of air and water using standard Schlenk

line and glovebox techniques under an argon or dinitrogen atmosphere. Solvents were sparged with UHP argon and dried by passage through columns containing Q-5 and molecular sieves prior to use. Elemental analyses were conducted on a PerkinElmer 2400 Series II CHNS elemental analyzer. Infrared spectra were collected on an Agilent Cary 630 spectrimeter equipped with a diamond ATR attachment. UV-visible spectra were collected in THF and Et₂O at room temperature in a 1 mm cell fitted with a Teflon stopcock using an Agilent Cary 60 UV-visible spectrophotometer. 2.2.2-Cryptand (crypt, Merck) was placed under vacuum (10⁻⁴ Torr) for 12 h before use. 18-Crown-6 (18-c-6, Alfa Aesar) was sublimed before use. TEMPO (98%, Sigma-Aldrich) was sublimed before use. CS₂ (Sigma-Aldrich) and pyridine (Sigma-Aldrich) were freeze-pump-thawed and stored over 3 Å molecular sieves for 1 week before use. BiPh3 (Alfa Aesar) was used as received. [K(18-c-6)₂][Gd(NR₂)₃] (1) and [K(crypt)][Gd(NR₂)₃] (2) were synthesized via literature proce-

{[K(18-c-6)](μ_3 -CS₃-κS,κ²S′,S′′)Gd(NR₂)₂]}₂ (3). In an Ar glovebox, [K(18-c-6)₂][Gd(NR₂)₃] (50 mg, 0.04 mmol) was dissolved in Et₂O (2 mL) chilled to -35 °C and excess CS₂ was added dropwise. The solution changed from dark blue to yellow. The solution was layered into cold hexanes and placed in a-35 °C freezer, producing a red oil and yellow crystals suitable for X-ray diffraction (6 mg, 8%). IR (cm⁻¹): 2890m, 1465w, 1352m, 1237m, 1102s, 943s, 827s, 767w, 696w, 661s. IR (cm⁻¹; red oil): 2889m, 1471w, 1351w, 1239m, 1105s, 945s, 823s, 765w, 696w, 662m. UV-vis in THF: λ_{max} 333 nm (ε = 3619 M⁻¹ cm⁻¹). Anal. Calcd for C₅₀H₁₂₂N₄O₁₂S₆Si₈K₂Gd₂: C, 33.71; H, 6.90; N, 3.15. Found: C, 33.68; H, 6.58; N, 2.71.

<code>[K(crypt)]{(R_2N)_2Gd[SCS(CH_2)Si(Me_2)N(SiMe_3)-\kappa N, \kappa S]}\$ (4). In an Ar glovebox, [K(crypt)][Gd(NR_2)_3] (50 mg, 0.05 mmol), was dissolved in THF (2 mL) chilled to $-35\,^{\circ}\text{C}$ and excess CS_2 was added dropwise. The solution turned from dark blue to yellow and was layered into cold hexanes and placed in a-35 $^{\circ}\text{C}$ freezer. A few yellow crystals suitable for X-ray diffraction were isolated. IR (cm $^{-1}$): 2948w, 2880w, 2812w, 2409w, 1475w, 1443w, 1397w, 1353m, 1295w, 1238m, 1150m, 1014w, 947m, 827m, 750w, 664w. Anal. Calcd for C $_{37}H_{90}N_5O_6S_2Si_6KGd$: C, 39.32; H, 8.03; N, 6.02. Found: C, 33.73; H, 7.83; N, 5.95. The low values indicate incomplete combustion, as has been previously observed in f-element chemistry. $^{75-82}$ </code>

 $\{[K(18-c-6)(NC_5H_5)_2]\}_2 \{[(R_2N)_3Gd]_2 [\mu-(NC_5H_4-C_5H_4N)_2]\} \ (5). \ \ In an argon-filled glovebox, [K(18-c-6)_2][Gd(NR_2)_3] \ (100 \ mg, 0.08 \ mmol) was dissolved in Et_2O (2 mL) chilled to <math display="inline">-35$ °C and excess pyridine, also chilled to -35 °C, was added dropwise. The solution turned from dark blue to light pink. The resulting solution was layered under cold hexanes and placed in a-35 °C freezer. Pink crystals suitable for X-ray diffraction were isolated (39 mg, 43%). IR (cm^-1): 2941w, 2889w, 1634w, 1453w, 1351w, 1237m, 1105s, 958s, 868m, 819s, 770m, 747m, 702w, 660m. Anal. Calcd for $C_{71}H_{168}N_8O_{12}Si_{12}K_2Gd_2$: C, 41.48; H, 8.24; N, 5.45. Found: C, 41.36; H, 8.23; N, 5.54.

<code>[K(crypt)]_2[[(NR_2)_3Gd]_2[\$\mu\$-(NC_5H_4-C_5H_4N)_2]\$ (6).</code> In an argonfilled glovebox, <code>[K(crypt)][Gd(NR_2)_3]\$ (100 mg, 0.09 mmol),</code> was dissolved in THF (2 mL) chilled to -35 °C and excess pyridine, chilled to -35 °C, was added dropwise. The solution turned from dark blue to light pink. The resulting solution was layered under cold hexanes and placed in a-35 °C freezer. Pink crystals suitable for X-ray diffraction were isolated (89 mg, 83%). IR (cm $^{-1}$): 2944w, 2882w, 2812w, 1637w, 1562w, 1476w, 1354w, 1236m, 1103m, 961m, 868m, 821m, 770m, 747m, 702w, 660m.

[K(18-c-6)][(R₂N)₃Gd(η^1 -ONC₅H₆Me₄)] (7). In an argon-filled glovebox, [K(18-c-6)₂][Gd(NR₂)₃] (50 mg, 0.05 mmol) was dissolved in Et₂O (2 mL) chilled to -35 °C. A solution of TEMPO (13 mg, 0.080 mmol) dissolved in Et₂O (2 mL) chilled to -35 °C was added dropwise to the dark blue solution of [K(18-c-6)₂][Gd(NR₂)₃]. The solution turned from dark blue to light pink. The resulting solution was layered under cold hexanes and placed in a-35 °C freezer. Colorless crystals suitable for X-ray diffraction were isolated (54 mg, 59%). IR (cm⁻¹): 2887m, 1470w, 1452w, 1352w, 1296w, 1106s, 956s, 864m, 824s, 770m, 700w, 660m.

[K(crypt)][(R₂N)₃Gd(η¹-ONC₅H₆Me₄)] (8). In an argon-filled glovebox, [K(crypt)][Gd(NR₂)₃] (100 mg, 0.09 mmol) was dissolved in THF (2 mL) chilled to -35 °C. A solution of TEMPO (14 mg, 0.090 mmol) dissolved in THF (2 mL) chilled to -35 °C was added dropwise to the dark blue solution of [K(crypt)][Gd(NR₂)₃]. The solution turned from dark blue to light pink. The resulting solution was layered under cold hexanes and placed in a -35 °C freezer. Colorless crystals suitable for X-ray diffraction were isolated (57 mg, 44%). IR (cm⁻¹): 2938w, 2885w, 2815w, 1477w, 1444w, 1354w, 1296w, 1235m, 1133w, 1104m, 1078w, 951s, 864m, 824s, 770m, 752m, 700w, 660m. Anal. Calcd for C₄₅H₁₀₈N₆O₇Si₆KGd: C, 44.66; H, 9.00; N, 6.94. Found: C, 44.99; H, 9.47; N, 6.80.

ASSOCIATED CONTENT

Supporting Information

The Supporting Information is available free of charge at https://pubs.acs.org/doi/10.1021/acs.inorgchem.1c02241.

Spectroscopic research and crystallographic information on complexes 3–10 (PDF)

Accession Codes

CCDC 2097994–2098005 contain the supplementary crystallographic data for this paper. These data can be obtained free of charge via www.ccdc.cam.ac.uk/data_request/cif, or by emailing data_request@ccdc.cam.ac.uk, or by contacting The Cambridge Crystallographic Data Centre, 12 Union Road, Cambridge CB2 1EZ, UK; fax: +44 1223 336033.

AUTHOR INFORMATION

Corresponding Author

William J. Evans — Department of Chemistry, University of California, Irvine, California 92697-2025, United States; orcid.org/0000-0002-0651-418X; Email: wevans@uci.edu

Authors

Amanda B. Chung — Department of Chemistry, University of California, Irvine, California 92697-2025, United States; orcid.org/0000-0001-8943-0303

Austin J. Ryan — Department of Chemistry, University of California, Irvine, California 92697-2025, United States; orcid.org/0000-0003-0983-0150

Ming Fang — Department of Chemistry, University of California, Irvine, California 92697-2025, United States Joseph W. Ziller — Department of Chemistry, University of California, Irvine, California 92697-2025, United States; orcid.org/0000-0001-7404-950X

Complete contact information is available at: https://pubs.acs.org/10.1021/acs.inorgchem.1c02241

Notes

The authors declare no competing financial interest.

ACKNOWLEDGMENTS

We thank the U.S. National Science Foundation for support of this research through grant CHE-1855328 (W.J.E.).

REFERENCES

(1) Hitchcock, P. B.; Lappert, M. F.; Maron, L.; Protchenko, A. V. Lanthanum Does Form Stable Molecular Compounds in the + 2 Oxidation State. *Angew. Chem., Int. Ed.* **2008**, 47 (47), 1488–1491.

(2) MacDonald, M. R.; Ziller, J. W.; Evans, W. J. Synthesis of a Crystalline Molecular Complex of Y²⁺, [(18-Crown-6)K]-[(C₃H₄SiMe₃)₃Y]. *J. Am. Chem. Soc.* **2011**, 133 (40), 15914–15917.

- (3) MacDonald, M. R.; Bates, J. E.; Fieser, M. E.; Ziller, J. W.; Furche, F.; Evans, W. J. Expanding Rare-Earth Oxidation State Chemistry to Molecular Complexes of Holmium(II) and Erbium(II). *J. Am. Chem. Soc.* **2012**, *134* (20), 8420–8423.
- (4) Macdonald, M. R.; Bates, E.; Ziller, J. W.; Furche, F.; Evans, W. J. Completing the Series of + 2 Ions for the Lanthanide Elements: Synthesis of Molecular Complexes of Pr⁺², Gd⁺², Tb⁺², and Lu⁺². J. Am. Chem. Soc. **2013**, 135, 9857–9868.
- (5) Evans, W. J. Tutorial on the Role of Cyclopentadienyl Ligands in the Discovery of Molecular Complexes of the Rare-Earth and Actinide Metals in New Oxidation States. *Organometallics* **2016**, *35*, 3088–3100.
- (6) Woen, D. H.; Evans, W. J. Expanding the + 2 Oxidation State of the Rare-Earth Metals, Uranium, and Thorium in Molecular Complexes. In *Handbook on the Physics and Chemistry of Rare Earths*; Elsevier: 2016; pp 1–57.
- (7) Fieser, M. E.; Macdonald, M. R.; Krull, B. T.; Bates, J. E.; Ziller, J. W.; Furche, F.; Evans, W. J. Structural, Spectroscopic, and Theoretical Comparison of Traditional vs Recently Discovered Ln^{2+} Ions in the $[K(2.2.2\text{-Cryptand})][(C_5H_4SiMe_3)_3Ln]$ Complexes: The Variable Nature of Dy^{2+} and Nd^{2+} . J. Am. Chem. Soc. **2015**, 137 (1), 369–382.
- (8) Kotyk, C. M.; MacDonald, M. R.; Ziller, J. W.; Evans, W. J. Reactivity of the ${\rm Ln}^{2+}$ Complexes [K(2.2.2-Cryptand)]-[(${\rm C_5H_4SiMe_3}$)₃Ln]: Reduction of Naphthalene and Biphenyl. *Organometallics* **2015**, 34 (11), 2287–2295.
- (9) Palumbo, C. T.; Fieser, M. E.; Ziller, J. W.; Evans, W. J. Reactivity of Complexes of 4fⁿ5d¹ and 4fⁿ⁺¹ Ln²⁺ Ions with Cyclooctatetraene. *Organometallics* **2017**, *36* (19), 3721–3728.
- (10) Ryan, A. J.; Darago, L. E.; Balasubramani, G.; Chen, G. P.; Ziller, J. W.; Furche, F.; Long, J. R.; Evans, W. J. Synthesis, Structure, and Magnetism of Tris(amide) [Ln{N(SiMe₃)₂}₃]¹⁻ Complexes of the Non-traditional + 2 Lanthanide Ions. *Chem. Eur. J.* **2018**, 24 (2), 7702–7709.
- (11) Ryan, A. J.; Ziller, J. W.; Evans, W. J. The Importance of the Counter-cation in Reductive Rare-Earth Metal Chemistry: 18-Crown-6 Instead of 2,2,2-Cryptand Allows Isolation of $[Y^{II}(NR_2)_3]^{1-}$ and Ynediolate and Enediolate Complexes from CO Reactions. *Chem. Sci.* 2020, 11 (11), 2006–2014.
- (12) Woen, D. H.; Chen, G. P.; Ziller, J. W.; Boyle, T. J.; Furche, F.; Evans, W. J. End-On Bridging Dinitrogen Complex of Scandium. *J. Am. Chem. Soc.* **2017**, *139*, 14861–14864.
- (13) Woen, D. H.; Chen, G. P.; Ziller, J. W.; Boyle, T. J.; Furche, F.; Evans, W. J. Solution Synthesis, Structure, and CO₂ Reduction Reactivity of a Scandium(II) Complex, {Sc(N(SiMe₃)₂]₃}⁻. Angew. Chem., Int. Ed. **2017**, 56, 2050–2053.
- (14) Ryan, A. J.; Balasubramani, S.; Ziller, J. W.; Furche, F.; Evans, W. J. Formation of the End-on Bound Lanthanide Dinitrogen Complexes, $[(R_2N)_3Ln-N=N-Ln(NR_2)_3]^{2-}$, from Divalent $[(R_2N)_3Ln]^{1-}$ Salts $(R=SiMe_3)$. J. Am. Chem. Soc. **2020**, 142 (20), 9302–9313.
- (15) Tilley, T. D.; Andersen, R. A.; Zalkin, A. Divalent Lanthanide Chemistry. Preparation and Crystal Structures of Sodium Tris[bis-(trimethylsilyl)amido]europate(II) and Sodium Tris[bis-(trimethylsilyl)amido]ytterbate(II), NaM[N(SiMe₃)₂]₃. *Inorg. Chem.* 1984, 23 (15), 2271–2276.
- (16) Evans, W. J.; Johnston, M. A.; Clark, R. D.; Anwander, R.; Ziller, J. W. Heteroleptic and Heterometallic Divalent Lanthanide Bis(Trimethylsilyl)Amide Complexes: Mixed Ligand, Inverse Sandwich, and Alkali Metal Derivatives. *Polyhedron* **2001**, 20 (19), 2483–2490.
- (17) Fang, M.; Farnaby, J. H.; Ziller, J. W.; Bates, J. E.; Furche, F.; Evans, W. J. Isolation of $(CO)^{1-}$ and $(CO2)^{1-}$ Radical Complexes of Rare Earths via $Ln(NR_2)_3/K$ Reduction and $[K_2(18\text{-Crown-6})_2]^{2+}$ Oligomerization. *J. Am. Chem. Soc.* **2012**, *134*, 6064–6067.
- (18) Werner, D.; Deacon, G. B.; Junk, P. C. Trapping $\mathrm{CS_2}^2$ and $\mathrm{S_3}^2$ between Two Ytterbium Formamidinates. *Inorg. Chem.* **2019**, 58 (3), 1912–1918.

- (19) Toniolo, D.; Willauer, A. R.; Andrez, J.; Yang, Y.; Scopelliti, R.; Maron, L.; Mazzanti, M. CS₂ Reductive Coupling to Acetylenedithiolate by a Dinuclear Ytterbium(II) Complex. *Chem. Eur. J.* **2019**, 25 (33), 7831–7834.
- (20) Heitmann, D.; Jones, C.; Mills, D. P.; Stasch, A. Low Coordinate Lanthanide(II) Complexes Supported by Bulky Guanidinato and Amidinato Ligands. *Dalt. Trans.* **2010**, *39* (7), 1877–1882.
- (21) Deacon, G. B.; Junk, P. C.; Wang, J.; Werner, D. Reactivity of Bulky Formamidinatosamarium(II or III) Complexes with C = O and C = S Bonds. *Inorg. Chem.* **2014**, *53* (23), 12553–12563.
- (22) Andrez, J.; Pøcaut, J.; Bayle, P.; Mazzanti, M. Tuning Lanthanide Reactivity Towards Small Molecules with Electron-Rich Siloxide Ligands. *Angew. Chem., Int. Ed.* **2014**, 53, 10448–10452.
- (23) Lam, O. P.; Castro, L.; Kosog, B.; Heinemann, F. W.; Maron, L.; Meyer, K. Formation of a Uranium Trithiocarbonate Complex via the Nucleophilic Addition of a Sulfide-Bridged Uranium Complex to CS₂. *Inorg. Chem.* **2012**, *51* (2), 781–783.
- (24) Camp, C.; Cooper, O.; Andrez, J.; Pécaut, J.; Mazzanti, M. CS₂ Activation at Uranium(III) Siloxide Ate Complexes: The Effect of a Lewis Acidic Site. *Dalt. Trans.* **2015**, 44 (6), 2650–2656.
- (25) Schneider, C.; Demeshko, S.; Meyer, F.; Werncke, C. G. A Molecular Low-Coordinate [Fe-S-Fe] Unit in Three Oxidation States. *Chem. Eur. J.* **2021**, 27 (20), 6348–6353.
- (26) Shannon, R. D. Revised Effective Ionic Radii and Systematic Studies of Interatomie Distances in Halides and Chaleogenides. *Acta Crystallogr., Sect. A: Cryst. Phys., Diffr., Theor. Gen. Crystallogr.* 1976, 32, 751–767.
- (27) Allen, F. H.; Kennard, O.; Watson, D. G.; Brammer, L.; Orpen, A. G.; Taylor, R. Tables of Bond Lengths Determined by X-Ray and Neutron Diffraction. Part 1. Bond Lengths in Organic Compounds. *J. Chem. Soc., Perkin Trans.* 1987, 2, S1–S19.
- (28) Aspinall, H. C.; Bradley, D. C.; Hursthouse, M. B.; Sales, K. D.; Walker, N. P. C. Lanthanide Thiolate Complexes: Synthesis of $[Ln{N(SiMe_3)_2}(\mu-SBu^t)]_2$ (Ln = Eu, Gd, Y) and the X-Ray Crystal Structure of the Gd Complex. *J. Chem. Soc., Chem. Commun.* **1985**, 2 (22), 1585–1586.
- (29) Simpson, S. J.; Turner, H. W.; Andersen, R. A. Hydrogen-Deuterium Exchange: Perdeuteriohydridotris-(Hexamethyldisilylamido)Thorium(IV) and-Uranium(IV). *J. Am. Chem. Soc.* 1979, 101 (26), 7728–7729.
- (30) Andersen, R. A. Chloro-and Methyltris[(Hexamethyldisilyl)-Amido]Zirconium(IV) and-Hafnium(IV). *Inorg. Chem.* **1979**, *18* (6), 1724–1725.
- (31) Han, F.; Zhang, J.; Yi, W.; Zhang, Z.; Yu, J.; Weng, L.; Zhou, X. γ -Deprotonation of Anionic Bis(Trimethylsilyl)Amidolanthanide Complexes with a Countered $[(Tp^{Me2})_2Ln]^+$ Cation. *Inorg. Chem.* **2010**, 49, 2793–2798.
- (32) Fortier, S.; Wu, G.; Hayton, T. W. Synthesis of a Nitrido-Substituted Analogue of the Uranyl Ion, $[N = U=O]^+$. *J. Am. Chem. Soc.* **2010**, *132* (20), 6888–6889.
- (33) Fang, M.; Bates, J. E.; Lorenz, S. E.; Lee, D. S.; Rego, D. B.; Ziller, J. W.; Furche, F.; Evans, W. J. $(N_2)^{3-}$ Radical Chemistry via Trivalent Lanthanide Salt/Alkali Metal Reduction of Dinitrogen: New Syntheses and Examples of $(N_2)^{2-}$ and $(N_2)^{3-}$ Complexes and Density Functional Theory Comparisons of Closed Shell Sc³⁺,Y³⁺, and Lu³⁺ versus 4f⁹ Dy³⁺. *Inorg. Chem.* **2011**, 50 (4), 1459–1469.
- (34) Fortier, S.; Kaltsoyannis, N.; Wu, G.; Hayton, T. W. Probing the Reactivity and Electronic Structure of a Uranium(V) Terminal Oxo Complex. *J. Am. Chem. Soc.* **2011**, *133* (36), 14224–14227.
- (35) Lewis, A. J.; Williams, U. J.; Carroll, P. J.; Schelter, E. J. Tetrakis(bis(trimethylsilyl)amido)uranium(IV): Synthesis and Reactivity. *Inorg. Chem.* **2013**, *52* (13), 7326–7328.
- (36) Smiles, D. E.; Wu, G.; Hayton, T. W. Reactivity of [U(CH₂SiMe₂NSiMe₃)(NR₂)₂] (R = SiMe₃) with Elemental Chalcogens: Towards a Better Understanding of Chalcogen Atom Transfer in the Actinides. *New J. Chem.* **2015**, 39 (10), 7563–7566.
- (37) Simpson, S. J.; Turner, H. W.; Andersen, R. A. Preparation and Hydrogen-Deuterium Exchange of Alkyl and Hydride Bis-

- (Trimethylsilyl)Amido Derivatives of the Actinide Elements. *Inorg. Chem.* **1981**, 20 (9), 2991–2995.
- (38) Moore, M.; Gambarotta, S.; Bensimon, C. Serendipitous Formation of a Dinuclear Vanadium(III) Amide Complex Containing a Vanadaazacyclobutane Ring. Potassium—Hydrogen Agostic Interactions Holding Together a V_2K_2 Tetrametallic Framework. *Organometallics* 1997, 16 (5), 1086–1088.
- (39) Galsworthy, J. R.; Green, M. L. H.; Müller, M. Synthesis and Crystal Structure of the Tris(amide) Cations [M{N(SiMe₃)₂}₃]⁺ (M = Zr or Hf): Evidence for M-Si-C Interactions. *J. Chem. Soc. Dalt. Trans.* 1998, 868, 387–392.
- (40) Karl, M.; Harms, K.; Seybert, G.; Massa, W.; Fau, S.; Frenking, G.; Dehnicke, K. Deprotonation Reactions of Silylated Amido Complexes of Rare Earth Elements. *Z. Anorg. Allg. Chem.* **1999**, 625 (12), 2055–2063.
- (41) Yu, X.; Bi, S.; Guzei, I. A.; Lin, Z.; Xue, Z. L. Zirconium, Hafnium, and Tantalum Amide Silyl Complexes: Their Preparation and Conversion to Metallaheterocyclic Complexes via γ-Hydrogen Abstraction by Silyl Ligands. *Inorg. Chem.* **2004**, *43* (22), 7111–7119.
- (42) Niemeyer, M. Reactions of Hypersilyl Potassium with Rare-Earth Metal Bis(Trimethylsilylamides): Addition versus Peripheral Deprotonation. *Inorg. Chem.* **2006**, *45* (22), 9085–9095.
- (43) Graves, C. R.; Schelter, E. J.; Cantat, T.; Scott, B. L.; Kiplinger, J. L. A Mild Protocol to Generate Uranium(IV) Mixed-Ligand Metallocene Complexes Using Copper(I) Iodide. *Organometallics* **2008**, *27* (20), 5371–5378.
- (44) Gardner, B. M.; McMaster, J.; Lewis, W.; Blake, A. J.; Liddle, S. T. A Crystallizable Dinuclear Tuck-in-Tuck-over Tuck-over Dialkyl Tren Uranium Complex and Double Dearylation of BPh₄⁻ to Give the BPh₂-Functionalized Metallocycle [U{N(CH₂CH₂NSiMe₃)₂(CH₂CH₂NSiMe₂CHBPh₂)}(THF)]. J. Am. Chem. Soc. **2009**, 131 (30), 10388–10389.
- (45) Corbey, J. F.; Woen, D. H.; Palumbo, C. T.; Fieser, M. E.; Ziller, J. W.; Furche, F.; Evans, W. J. Ligand Effects in the Synthesis of Ln²⁺ Complexes by Reduction of Tris(cyclopentadienyl) Precursors Including C-H Bond Activation of an Indenyl Anion. *Organometallics* **2015**, 34 (15), 3909–3921.
- (46) Jaroschik, F.; Momin, A.; Nief, F.; Le Goff, X.-F.; Deacon, G. B.; Junk, P. C. Dinitrogen Reduction and C-H Activation by the Divalent Organoneodymium Complex $[C_5H_2tBu_3)_2Nd(\mu-I)K([18]-Crown-6]$. *Angew. Chemie Int. Ed.* **2009**, 48, 1117–1121.
- (47) Fieser, M. E.; Palumbo, C. T.; La Pierre, H. S.; Halter, D. P.; Voora, V. K.; Ziller, J. W.; Furche, F.; Meyer, K.; Evans, W. J. Comparisons of Lanthanide/Actinide + 2 Ions in a Tris(Aryloxide)-Arene Coordination Environment. *Chem. Sci.* **2017**, 8 (11), 7424–7433.
- (48) van den Hende, J. R.; Hitchcock, P. B.; Lappert, M. F. Reaction of Ytterbim(II) Amides with Various Bronsted Acids, CS_2 or LiNR₂; Crystal Structures of $[\{Yb(NR_2)(\mu\text{-}OCBu^t_3)\}_2]$ and $[Yb-(OCBu^t_3)_2(thf)_2]$ (R = SiMe₃, thf = Tetrahydrofuran). *J. Chem. Soc. Dalt. Trans.* 1995, 2251–2258.
- (49) Labouille, S.; Nief, F.; Le Goff, X. F.; Maron, L.; Kindra, D. R.; Houghton, H. L.; Ziller, J. W.; Evans, W. J. Ligand Influence on the Redox Chemistry of Organosamarium Complexes: Experimental and Theoretical Studies of the Reactions of $(C_5Me_5)_2Sm(THF)_2$ and $(C_4Me_4P)_2Sm$ with Pyridine and Acridine. *Organometallics* **2012**, 31 (14), 5196–5203.
- (50) Fedushkin, I. L.; Nevodchikov, V. I.; Bochkarev, M. N.; Dechert, S.; Schumann, H. Reduction of 2,5-di-*tert*butylcyclopenta-dienone and Pyridine with Thulium Diiodide. Structures of the Complexes $TmI_2(THF)_2[\eta^5-Bu^t_2C_5H_2O]TmI_2(THF)_3$ and $[TmI_2(C_5H_5N)_4]_2(\mu_2-N_2C_{10}H_{10})$. Russ. Chem. Bull. **2003**, 52 (1), 154–159.
- (51) Jaroschik, F.; Nief, F.; Le Goff, X. F.; Ricard, L. Synthesis and Reactivity of Organometallic Complexes of Divalent Thulium with Cyclopentadienyl and Phospholyl Ligands. *Organometallics* **2007**, *26* (14), 3552–3558.
- (52) Mazzanti, M.; Modder, D. K.; Palumbo, C. T.; Douair, I.; Fadaei-Tirani, F.; Maron, L. Delivery of a Masked Uranium(II) by an

- Oxide-Bridged Diuranium(III) Complex. Angew. Chem., Int. Ed. 2021, 60, 3737.
- (53) Formanuik, A.; Ortu, F.; Liu, J.; Nodaraki, L. E.; Tuna, F.; Kerridge, A.; Mills, D. P. Double Reduction of 4,4'-Bipyridine and Reductive Coupling of Pyridine by Two Thorium(III) Single-Electron Transfers. *Chem. Eur. J.* **2017**, 23 (10), 2290–2293.
- (54) Dugan, T. R.; Bill, E.; MacLeod, K. C.; Christian, G. J.; Cowley, R. E.; Brennessel, W. W.; Ye, S.; Neese, F.; Holland, P. L. Reversible C-C Bond Formation between Redox-Active Pyridine Ligands in Iron Complexes. *J. Am. Chem. Soc.* **2012**, *134* (50), 20352–20364.
- (55) Demir, S.; Gonzalez, M. I.; Darago, L. E.; Evans, W. J.; Long, J. R. Giant Coercivity and High Magnetic Blocking Temperatures for N_2^{3-} Radical-Bridged Dilanthanide Complexes upon Ligand Dissociation. *Nat. Commun.* **2017**, *8*, 1–9.
- (56) Bartholomew, A. K.; Teesdale, J. J.; Sanchez, R. H.; Malbrecht, B. J.; Jude, C. E.; Menard, G.; Bu, W.; Iovan, D. A.; Mikhailine, A. A.; Zheng, S.-L.; Sarangi, R.; Wang, S. G.; Chen, Y.-S.; Betley, T. A. CCDC 1897928: Experimental Crystal Structure Determination. CSD Communication, 2019.
- (57) Langeslay, R. R.; Walensky, J. R.; Ziller, J. W.; Evans, W. J. Reactivity of Organothorium Complexes with TEMPO. *Inorg. Chem.* **2014**, *53* (16), 8455–8463.
- (58) Farnaby, J. H.; Fang, M.; Ziller, J. W.; Evans, W. J. Expanding Yttrium Bis(Trimethylsilylamide) Chemistry through the Reaction Chemistry of $(N_2)^2$, $(N_2)^3$, and $(NO)^2$ Complexes. *Inorg. Chem.* **2012**, *51* (20), 11168–11176.
- (59) Dickman, M. H.; Doedens, R. J. Structure of Chloro(2,2,4,4-Tetramethylpiperidinyl-1-Oxo-O,N)(Triphenylphosphine)Palladium-(II), a Metal Complex of a Reduced Nitroxyl Radical. *Inorg. Chem.* **1982**, 21 (2), 682–684.
- (60) Mahanthappa, M. K.; Huang, K. W.; Cole, A. P.; Waymouth, R. M. Synthesis and Molecular Structure of Titanium Complexes Containing a Reduced TEMPO Radical. *Chem. Commun.* **2002**, 2 (5), 502–503.
- (61) Evans, W. J.; Perotti, J. M.; Doedens, R. J.; Ziller, J. W. The Tetramethylpiperidinyl-1-oxide Anion (TMPO⁻) as a Ligand in Lanthanide Chemistry: Synthesis of the per(TMPO⁻) Complex-[(ONC₅H₆Me₄)₂Sm(μ-ONC₅H₆Me₄)]₂. *Chem. Commun.* **2001**, 1 (22), 2326–2327.
- (62) Jaitner, P.; Huber, W.; Hunter, G.; Scheidsteger, O. Synthesis and X-Ray Structure of (2,2,6,6-Tetramethyl-Piperidinyl-1-Oxo-O,N)Tricarbonylmanganese(0); "Side-on" Coordination of the Nitroxyl Radical to Manganese. *J. Organomet. Chem.* **1983**, 259 (1), C1–C5.
- (63) Westerhausen, M.; Weinrich, S.; Schmid, B.; Schneiderbauer, S.; Suter, M.; Noth, H.; Piotrowski, H. Synthesis, Spectroscopic Characterization, and Molecular Structures of Selected Lewis-Base Adducts of the Alkali Metal Tri(Tert-Butyl)Silylphosphanides. Z. Anorg. Allg. Chem. 2003, 629 (4), 625–633.
- (64) Likhar, P. R.; Zirngast, M.; Baumgartner, J.; Marschner, C. Preparation and Structural Characterisation of Methoxybis-(Trimethylsilyl)Silyl Potassium and Its Condensation Product. *Chem. Commun.* **2004**, *4* (15), 1764–1765.
- (65) Zitz, R.; Hlina, J.; Arp, H.; Kinschel, D.; Marschner, C.; Baumgartner, J. Group 4 Metal and Lanthanide Complexes in the Oxidation State + 3 with Tris(Trimethylsilyl)Silyl Ligands. *Inorg. Chem.* **2019**, *58* (10), 7107–7117.
- (66) Evans, W. J.; Giarikos, D. G.; Workman, P. S.; Ziller, J. W. Utility of Anhydrous Neodymium Nitrate as a Precursor to Extended Organoneodymium Nitrate Networks. *Inorg. Chem.* **2004**, *43* (18), 5754–5760.
- (67) Evans, W. J.; Gonzales, S. L.; Ziller, J. W. Organosamarium-Mediated Synthesis of Bismuth Bismuth Bonds: X-Ray Crystal Structure of the First Dibismuth Complex Containing a Planar $M_2(\mu \eta^2:\eta^2-\text{Bi}_2)$ Unit. J. Am. Chem. Soc. 1991, 113 (26), 9880–9882.
- (68) Ababei, R.; Massa, W.; Weinert, B.; Pollak, P.; Xie, X.; Clérac, R.; Weigend, F.; Dehnen, S. Ionic-Radius-Driven Selection of the Main-Group-Metal Cage for Intermetalloid Clusters [Ln@Pb_xBi_{14-x}]^{q-}

- and [Ln@Pb_yBi_{13-y}]^{q-} (x/q = 7/4, 6/3; y/q = 4/4, 3/3. *Chem. Eur. J.* **2015**, 21 (1), 386–394.
- (69) Rookes, T. M.; Wildman, E. P.; Balázs, G.; Gardner, B. M.; Wooles, A. J.; Gregson, M.; Tuna, F.; Scheer, M.; Liddle, S. T. Actinide—Pnictide (An—Pn) Bonds Spanning Non-Metal, Metalloid, and Metal Combinations (An = U, Th; Pn = P, As, Sb, Bi). *Angew. Chem., Int. Ed.* **2018**, *57* (5), 1332–1336.
- (70) Kindra, D. R.; Casely, I. J.; Fieser, M. E.; Ziller, J. W.; Furche, F.; Evans, W. J. Insertion of CO2 and COS into Bi-C Bonds: Reactivity of a Bismuth NCN Pincer Complex of an Oxyaryl Dianionic Ligand, [2,6-(Me₂NCH₂)₂C₆H₃]Bi(C₆H₂^tBu₂O). *J. Am. Chem. Soc.* **2013**, *135* (20), 7777–7787.
- (71) Silvestru, C.; Breunig, H. J.; Althaus, H. Structural Chemistry of Bismuth Compounds. I. Organobismuth Derivatives. *Chem. Rev.* **1999**, 99 (11), 3277–3327.
- (72) Birchall, T.; Vetrone, J. A. On the Structure of Alkali Metal Triphenylstannide Salts in Solution and in the Solid State. *J. Chem. Soc., Chem. Commun.* 1988, 877–879.
- (73) Englich, U.; Ruhlandt-Senge, K.; Uhlig, F. Novel Triphenyltin Substituted Derivatives of Heavier Alkaline Earth Metals. *J. Organomet. Chem.* **2000**, *613* (2), 139–147.
- (74) Reed, D.; Stalke, D.; Wright, D. S. Observation of a direct Sn-Li bond; the crystal and molecular structure of monomeric [Ph₃SnLi · PMDETA] and the detection of ^{119, 117}Sn-⁷Li NMR coupling in solution. *Angew. Chem., Int. Ed. Engl.* **1991**, *30* (11), 1459–1460.
- (75) Jenkins, T. F.; Woen, D. H.; Mohanam, L. N.; Ziller, J. W.; Furche, F.; Evans, W. J. Tetramethylcyclopentadienyl Ligands Allow Isolation of Ln(II) Ions across the Lanthanide Series in [K(2.2.2-Cryptand)][(C₅Me₄H)₃Ln] Complexes. *Organometallics* **2018**, 37 (21), 3863–3873.
- (76) Chilton, N. F.; Goodwin, C. A. P.; Mills, D. P.; Winpenny, R. E. P. The First Near-Linear Bis(Amide) f-Block Complex: A Blueprint for a High Temperature Single Molecule Magnet. *Chem. Commun.* **2015**, *51* (1), 101–103.
- (77) Goodwin, C. A. P.; Chilton, N. F.; Vettese, G. F.; Moreno Pineda, E.; Crowe, I. F.; Ziller, J. W.; Winpenny, R. E. P.; Evans, W. J.; Mills, D. P. Physicochemical Properties of Near-Linear Lanthanide(II) Bis(Silylamide) Complexes (Ln = Sm, Eu, Tm, Yb). *Inorg. Chem.* **2016**, *55* (20), 10057–10067.
- (78) Ortu, F.; Packer, D.; Liu, J.; Burton, M.; Formanuik, A.; Mills, D. P. Synthesis and Structural Characterization of Lanthanum and Cerium Substituted Cyclopentadienyl Borohydride Complexes. *J. Organomet. Chem.* **2018**, 857, 45–51.
- (79) Huh, D. N.; Roy, S.; Ziller, J. W.; Furche, F.; Evans, W. J. Isolation of a Square-Planar Th(III) Complex: Synthesis and Structure of [Th(OC₆H₂^tBu₂-2,6-Me-4)₄]¹⁻. *J. Am. Chem. Soc.* **2019**, 141 (32), 12458–12463.
- (80) Gabbaï, F. P.; Chirik, P. J.; Fogg, D. E.; Meyer, K.; Mindiola, D. J.; Schafer, L. L.; You, S. L. An Editorial about Elemental Analysis. *Organometallics* **2016**, *35* (19), 3255–3256.
- (81) Moehring, S. A.; Miehlich, M.; Hoerger, C. J.; Meyer, K.; Ziller, J. W.; Evans, W. J. A Room-Temperature Stable Y(II) Aryloxide: Using Steric Saturation to Kinetically Stabilize Y(II) Complexes. *Inorg. Chem.* **2020**, *59* (5), 3207–3214.
- (82) Goodwin, C. A. P.; Reta, D.; Ortu, F.; Chilton, N. F.; Mills, D. P. Synthesis and Electronic Structures of Heavy Lanthanide Metallocenium Cations. *J. Am. Chem. Soc.* **2017**, *139* (51), 18714–18724.